Switching Time Bifurcations in a Thyristor Controlled Reactor

Sasan Jalali, Ian Dobson, Robert H. Lasseter, and Giri Venkataramanan

Abstract—**Thyristor controlled reactors are high power switching circuits used for static VAR control and the emerging technology of flexible ac transmission. The static VAR control circuit considered in the paper is a nonlinear periodically operated RLC circuit with a sinusoidal source and ideal thyristors with equidistant firing pulses. This paper describes new instabilities in the circuit in which thyristor turn off times jump or bifurcate as a system parameter varies slowly. The new instabilities are called switching time bifurcations and are fold bifurcations of zeros of thyristor current. The bifurcation instabilities are explained and verified by simulation and an experiment. Switching time bifurcations are special to switching systems and, surprisingly, are not conventional bifurcations. In particular, switching time bifurcations cannot be predicted by observing the eigenvalues of the system Jacobian. We justify these claims by deriving a simple formula for the Jacobian of the Poincaré map of the circuit and presenting theoretical and numerical evidence that conventional bifurcations do not occur.**

I. Introduction

We study the stability of a high power switching circuit with a thyristor controlled reactor. This nonlinear circuit can exhibit novel bifurcation instabilities and our main objective is to explain and verify the new instabilities using simulation and experiment. A state space approach is used to derive a simple formula for the Jacobian of the Poincaré map of the circuit and confirm the nature of the new instabilities.

A thyristor controlled reactor is a fixed inductor in series with two oppositely poled thyristors as shown in the right most branch of Fig. 1. Controlling the firing (switch on) of the thyristors controls the thyristor conduction time and hence the proportion of time for which the inductor is included in the circuit. One approximation which is often used to understand the thyristor controlled reactor in a periodic steady state is that it acts as a continuously variable inductor. The value of the inductance depends on the thyristor conduction time. The thyristor controlled reactor is often combined with a fixed capacitor in parallel so that varying the thyristor conduction time varies the effective impedance of the parallel combination.

Manuscript received June 5, 1993. This work was supported in part by the Electric Power Research Institute under Contracts RP4000-29, RP8010-30, RP8050-03, RP8050-04, WO8050-03 and by the NSF Presidential Young Investigator Grant ECS-9157192. This paper was recommended by Associate Editor M. Ilic.

S. Jalali is with Siemens Energy and Automation, Atlanta, GA 30202 USA.

I. Dobson and R. H. Lasseter are with the Department of Electrical and Computer Engineering, University of Wisconsin, Madison, WI 53706 USA.

G. Venkataramanan is with the Department of Electrical Engineering, Montana State University, Bozeman, MT 59707 USA.

Publisher Item Identifier S 1057-7122(96)01665-0.

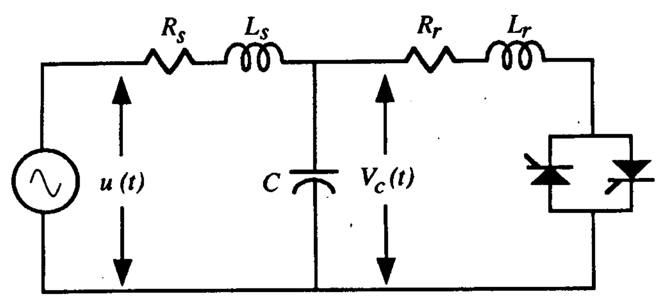

Fig. 1. Single phase static VAR system.

Since the mid-1970's, thyristor controlled reactors have been used at the loaded ends of transmission lines to control the reactive power supplied from a fixed shunt capacitor so that voltage can be maintained when system loads or transmission line configurations change [11], [20]. More recently, thyristor controlled reactors have been used as one of the economical alternatives for the emerging technology of flexible ac transmission (FACTS) [2]. The expected benefits of flexible ac transmission include increased and controllable power flows on transmission lines and the enhancement of power system stability.

Despite the significance of high power circuits with thyristor controlled reactors, little nonlinear theory has been developed for their analysis. The standard approach is to replace the thyristor controlled reactor by an average inductor model and then apply linear techniques to the resulting circuit [11], [20]. While this average inductor approximation is sometimes effective for predicting steady state behavior, it fails to capture much of the circuit nonlinearity and it breaks down when large harmonic distortions occur. Operating conditions with large harmonic distortions are documented in [1], [12], [27], [13]. While detailed time domain simulation is valuable in analyzing nonlinear effects in thyristor controlled reactor circuits, there is also a need to develop mathematical concepts and approaches so that the simulated or actual nonlinear phenomena may be understood and predicted.

This paper describes new instabilities of a thyristor controlled reactor circuit called switching time bifurcations in which thyristor switch off times jump or bifurcate as a parameter is slowly varied. The thyristor controlled reactor circuit and its classical operation are described in Sections II and III. The large harmonic distortions associated with switching time bifurcations are briefly summarized in Section IV. Sections V and VI explain that switching time bifurcations are fold bifurcations of the zeros of the thyristor current. Sec-

1057-7122/96$05.00 © 1996 IEEE

tion VII presents simulations of a thyristor controlled reactor circuit for static VAR control which shows switching time bifurcations in detail. The circuit was developed by Bohmann and Lasseter to study harmonic interactions and distortions [1]. This simulation evidence for switching time bifurcations is followed in Section VIII by experimental work showing switching time bifurcations on a single phase equivalent of the static VAR compensator installed near Rimouski, Quebec [20].

The occurrence of switching time bifurcations raises expectations that they should be related to well known generically occurring bifurcations. It is interesting that this is not the case and that switching time bifurcations appear to be a novel mechanism for instability. In particular, the occurrence of the switching time bifurcations cannot be predicted from eigenvalues of the system Jacobian. The remainder of the paper is devoted to explaining how the special properties of the thyristor controlled reactor circuit precludes conventional bifurcations. Sections IX, X, and XI compute the Poincaré map [10], [25] of the circuit and the Jacobian of the Poincaré map. The formula for this Jacobian is simplified considerably by the special properties of the thyristor turn off and is the same formula that would be obtained for fixed turn off times. Section XII computes the eigenvalues of the Jacobian to show that conventional bifurcations do not occur and explains how the Jacobian simplification ensures that switching time bifurcations are not predicted by the eigenvalues of the Jacobian. This paper differs from the initial conference paper [14] by including experimental results and reworked theory.

We briefly review other approaches to bifurcations in switching circuits. Switching circuits with high switching rates and ideal switches are well approximated using averaging methods [19], [17], [23] and the stability of the averaged system can be investigated using bifurcation theory [21], [24]. The high power switching circuits addressed in this paper have switching rates comparable to the 60 Hz frequency of the voltage sources and averaging methods have not been shown to be applicable. There are also simple low power switching circuit models that exhibit bifurcations and chaos when the nonlinear junction capacitance of a diode is modeled [4], [3].

In deriving the Jacobian of the Poincaré map, we use a state space analysis of switching circuits which overlaps with contributions of other authors. The fundamental work of Louis [18] computes Poincaré maps for switching circuits including controls. The varying dimensions of the state vector and switching conditions are discussed and formulas for the propagation of first order deviations through switchings are stated. The formulas show that Louis had used the Jacobian simplification which is highlighted in Section X. Louis computes as an example the Jacobian of the Poincaré map of an ac/dc convertor with a current regulator. Verghese *et al.* [26] give a general approach to computing Poincaré maps and their Jacobians for switching circuits. Circuit controls and symmetries and the automation of the computations are discussed but the Jacobian simplification and the varying dimension of the state vector are not treated. The linearized dynamics of a series resonant convertor are computed and studied. Grotzbach and Lutz [9] computed Jacobians of Poincaré maps of switched circuits including control actions. They develop Newton algorithms for computing steady state solutions and compute eigenvalues for ac/dc convertors with controls. The extension to nonlinear circuits and the derivation of averaged circuit models are discussed. Dobson [6] derives the Jacobian of a general switching circuit with RLC elements and ideal diodes or thyristors with an emphasis on the Jacobian simplification.

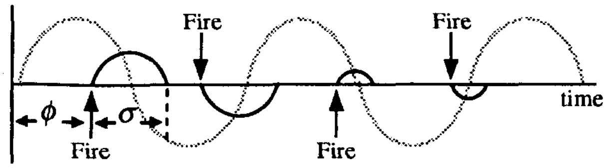

Fig. 2. Classical operation of thyristor controlled reactor.

The work in this paper has stimulated further work on the thyristor controlled reactor circuit such as its novel transient dynamics [22] and analyzing damping and resonance phenomena [5]. The effects of thyristor firing synchronization schemes on the Jacobian are computed and presented in [16], [15].

II. System Description

Fig. 1 shows a single phase static VAR compensator consisting of a thyristor controlled reactor and a parallel capacitor. The controlled reactor is modeled as a series combination of an inductor L_r and resistance R_r. The static VAR compensator is connected to an infinite bus behind a power system impedance of an inductance L_s and a resistance R_s in series.

The switching element of the thyristor controlled reactor consists of two oppositely poled thyristors which conduct on alternate half cycles of the supply frequency. A thyristor conducts current only in the forward direction, can block voltage in both directions, turns on when a firing pulse is provided and turns off when the thyristor current becomes zero. (The phenomenon of thyristor misfire [22] is not addressed here.) The thyristors are assumed ideal so that detailed nonlinearities in the turn on/off of the thyristors are neglected. The dependence of the thyristor switch off times on the system state causes circuit nonlinearity. The firing pulses are supplied periodically and the system is controlled by varying the phase ϕ (delay) of the firing pulses. The system is studied with the phase as an open loop control parameter. In practice a closed loop control would modify the firing phase.

III. Classical Analysis

The classical, idealized operation of a thyristor controlled reactor is explained in Fig. 2. In this figure, the gray line represents the thyristor controlled reactor voltage $V_c(t)$ (cf. Fig. 1) and the solid line represents the thyristor current.

If the thyristors are fired at the point where the voltage $V_c(t)$ is at a peak, full conduction results. The circuit then operates as if the thyristors were shorted out, resulting in a current which lags the voltage by 90°. If the firing is delayed from the peak voltage, the current becomes discontinuous with a reduced fundamental component of reactive current and a reduced thyristor conduction time σ. As the phase angle ϕ ranges between 90° and 180° the thyristor conduction time σ

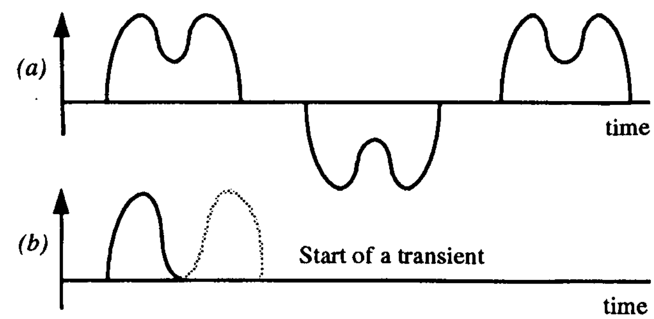

Fig. 3. Appearance of a new thyristor current zero. (a) $\phi < \phi^*$. (b) $\phi = \phi^*$.

ranges between 180° and 0°. The classical analysis assumes that the voltage $V_c(t)$ is a pure sinusoid.

IV. Harmonic Distortion

The classical analysis is often applicable, but can, as demonstrated here and in [1] and [12], fail for certain circuit parameters and operating conditions. Under these conditions, both the voltage and the current waveforms become greatly distorted with large harmonic components. This distortion is associated with a resonance phenomenon in which the natural frequencies of the circuit, from when the reactor is fully on to when it is fully off, span an odd harmonic [1], [5]. This harmonic distortion can lead to instabilities as switching times suddenly change or bifurcate as follows. It is useful to recall that fold bifurcations (also called saddle node bifurcations) can either create or annihilate pairs of zeros of functions or vector fields [10], [25].

V. Instability when a New Thyristor Current Zero Appears

Fig. 3 describes one way in which the system can lose stability. Suppose that harmonic distortion produces a fold or dip in the thyristor current as shown in Fig. 3(a). As the phase delay ϕ of the firing pulses slowly increases, the fold lowers until, passing through the critical phase ϕ^*, a new, earlier zero of the thyristor current is produced by a fold bifurcation of the thyristor current as shown in Fig. 3(b). (The new zero of the thyristor current in Fig. 3(b) is in fact a double zero.) The thyristor switching off time has suddenly decreased and the stable operation of the system at the previous periodic orbit has been lost. We call this qualitative change a switching time bifurcation. As soon as the switching time bifurcates, a transient starts.

VI. Instability when a Thyristor Current Zero Disappears

Fig. 4 explains another type of switching time bifurcation in which the system loses stability as a thyristor current zero disappears. Fig. 4(a) shows a periodic solution for the thyristor current with the solid line. The gray line shows the thyristor current that would occur if the thyristor did not switch off for negative current. This part of the current is referred to here as "virtual". The virtual current does not occur in circuit operation but it is useful in understanding how the current

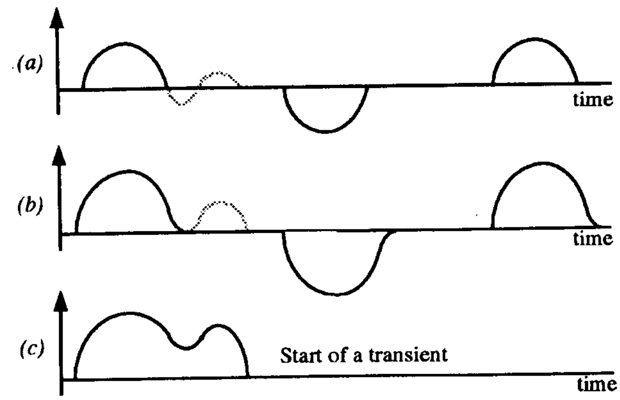

Fig. 4. Disappearance of a thyristor current zero. (a) $\phi < \phi^*$. (b) $\phi = \phi^*$. (c) $\phi > \phi^*$.

zero disappears. As the phase delay of the firing pulses slowly increases, the fold in the dotted line rises until, passing through the critical phase ϕ^*, the current zero disappears and a later zero of the thyristor current applies (see Fig. 4(b) and (c)). The switching off time of the thyristor has suddenly increased in a switching time bifurcation and stability has suddenly been lost. Note how the zero of the actual thyristor current coalesces with a zero of the virtual current indicated by the dotted line and disappears in a fold bifurcation. As soon as the switching time bifurcates and system stability is lost, a transient starts.

VII. Simulation Results

The switching time bifurcations are illustrated with the single phase static VAR circuit of Fig. 1 described in [1]. On a 1 MVA, 1 kV base, the source impedance has a per-unit magnitude of 7.35% with an angle of 89°, the reactor is a series combination of 62.6% inductive reactance and a 3.13% resistance. The capacitor bank has a capacitive reactance of 177%. Alternatively, the per unit component values can be specified as L_s =0.195 mH, R_s =0.9 mΩ, L_r =1.66 mH, R_r =31.3 mΩ, and C =1.5 mF. The firing pulses are equidistant and the phase ϕ is the relative phase of the firing pulses with respect to the stiff ac source $u(t) = \sin \omega t$ shown in Fig. 1. σ denotes the conduction time of the thyristors.

In this example, the system impedance and the capacitor bank have a natural frequency which is 4.9 times the fundamental frequency 60 Hz. If the controlled reactor is included in the circuit, the natural frequency shifts to 5.18 times the fundamental frequency. Thus the natural frequencies of the circuit from when the reactor is fully on to when it is fully off span the fifth harmonic. This crossing of an odd harmonic indicates that system odd harmonics can be large and that voltage and current wave forms can be significantly distorted [1], [5].

Fig. 5 shows how the conduction time σ of periodic orbits varies as the phase ϕ is varied. To simplify the calculations, only periodic orbits which are half wave symmetric are computed, using (16) and (17) from Section XI. As can be seen, two separate sets of periodic solutions are computed. One set starts at $\sigma = 180^o$ and ends at $\sigma \approx 91^o$. The other starts at $\sigma = 0^o$ and ends at $\sigma \approx 60^o$. The classical model predicts

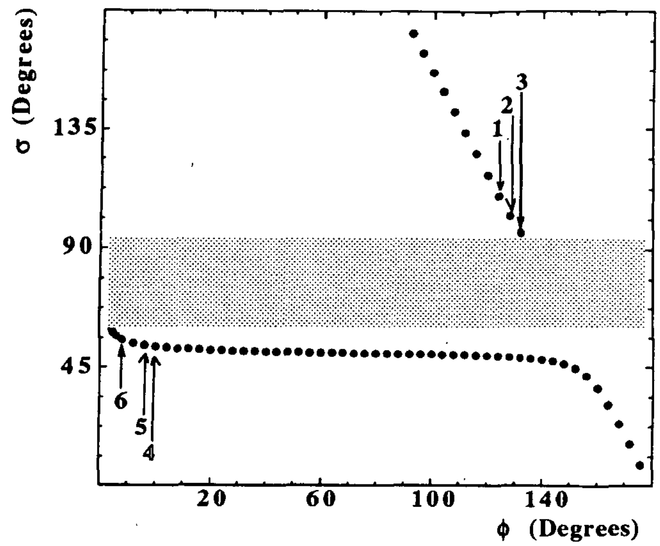

Fig. 5. Conduction time σ versus firing delay ϕ.

only one set of solutions starting from $\sigma = 0^o$ and ending at $\sigma = 180^o$.

In order to investigate how the system loses stability when stable periodic orbits disappear, the ElectroMagnetic Transient Program (EMTP) was used [7], [8]. Periodic orbits 1 through 6 in Fig. 5 were chosen to study in detail how harmonic distortion can cause periodic solutions to disappear in switching time bifurcations.

The loss of a stable periodic solution at σ near 91° is a switching time bifurcation in which a new thyristor current zero appears. The EMTP simulation in Fig. 6(a)–(c) shows periodic solutions of the thyristor current at periodic orbits 1, 2, and 3 respectively. Note that as we move toward periodic orbit 3, the harmonic distortion produces a fold in the thyristor current. Fig. 6(c) shows that as the phase delay of the firing pulses is slightly increased, the fold in the thyristor current lowers and a new, earlier zero of the thyristor current is produced and a transient starts.

The loss of a stable periodic solution at σ near 60° is a switching time bifurcation in which a thyristor current zero disappears. Fig. 7 shows how the periodic solutions behave as the switching time bifurcation is approached. The plots in Fig. 7 are on an expanded time scale so as to closely observe the behavior of the thyristors as they turn off. The dotted lines show the virtual current which would have occurred if the thyristors did not turn off as the current decreased through zero. As the phase is decreased, the periodic orbit progresses through periodic orbits 4, 5, and 6 and the zeros of the virtual and the actual current approach each other, coalesce, and disappear. The stable periodic solution disappears when the actual current zero disappears and the switch off time of the thyristor suddenly increases. The initial portion of the transient which occurs when the stable periodic solution disappears is shown in Fig. 8. The system will eventually converge slowly to another stable periodic solution.

Even though many systems enforce equidistant firing in steady state operation, the firing pulses may or may not

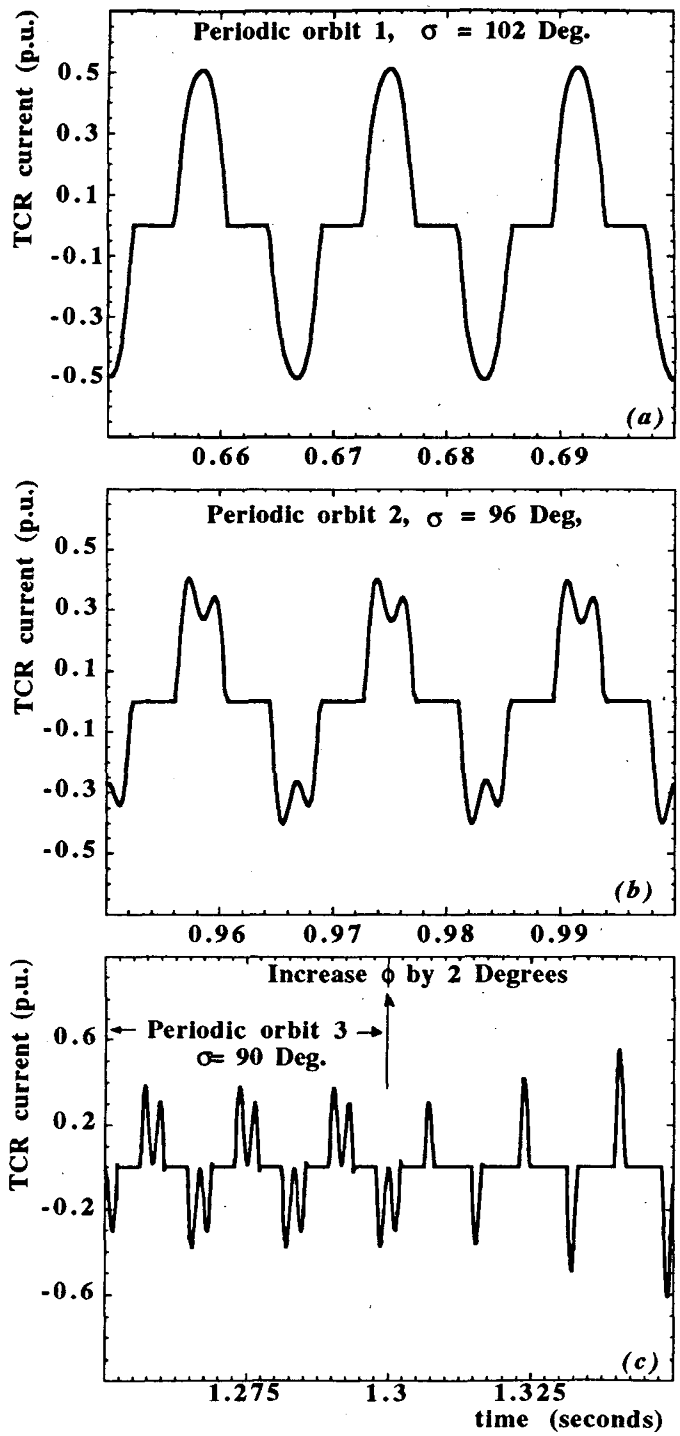

Fig. 6. A new thyristor current zero appears. (a) periodic orbit 1. (b) Periodic orbit 2. (c) Periodic orbit 3 up to 1.3 s. ϕ is increased by 2° at 1.3 s.

be equidistant during transients. Therefore, the detail of the transient depends heavily on the assumptions used in modeling the control of the thyristor firing pulses. The intent of the simulation results is to show the existence of the transient as a consequence of the switching time bifurcation rather than the detail of the transient. However, the computations of steady state periodic orbits as in Fig. 5 are valid for any firing control scheme that enforces equidistant firings in steady state.

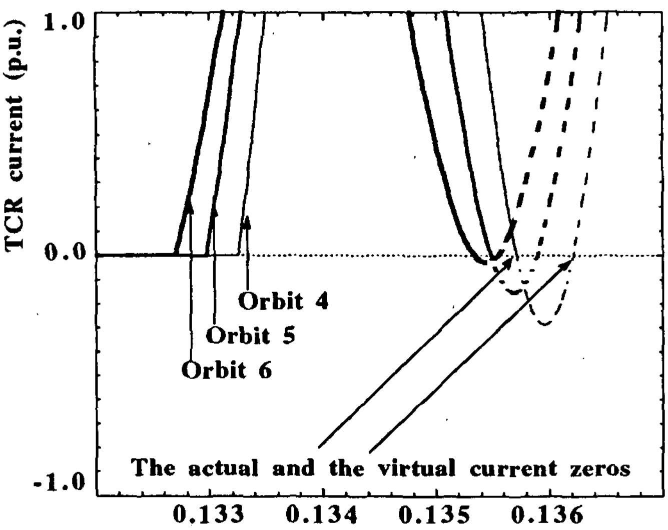

Fig. 7. Thyristor current on an expanded time scale for periodic orbits 4, 5, and 6.

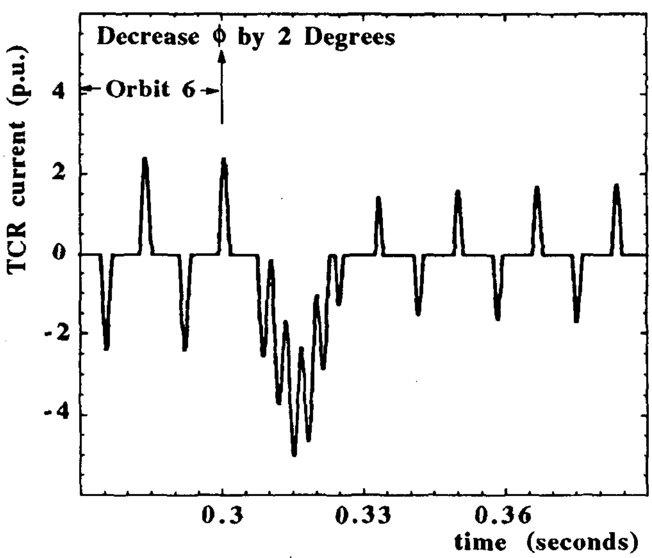

Fig. 8. Two current zeros coalesce and disappear. Periodic orbit 6 up to 0.3 s. ϕ is decreased by 2° at 0.3 s.

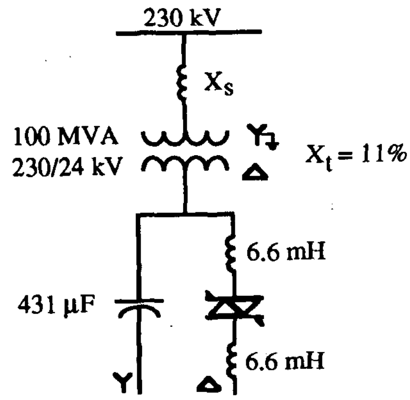

Fig. 9. Rimouski static VAR compensator.

TABLE I
RIMOUSKI AND EXPERIMENTAL CIRCUIT COMPONENTS

Data	Rimouski(3ϕ)	Experiment(1ϕ)
$V_{LL}(V_{LN})$	230 (132.8) kV	115.0 V
Power	100 MVA	301.4 VA
Z_{base}	529 Ω	43.88 Ω
X_{cap}(1.07 p.u.)	566 Ω	46.95 Ω
X_{tcr}(0.288 p.u.)	152.3 Ω	12.64 Ω
X_t(0.11 p.u.)	58.2 Ω	4.83 Ω
X_s(0.016 p.u.)	8.46 Ω	0.70 Ω

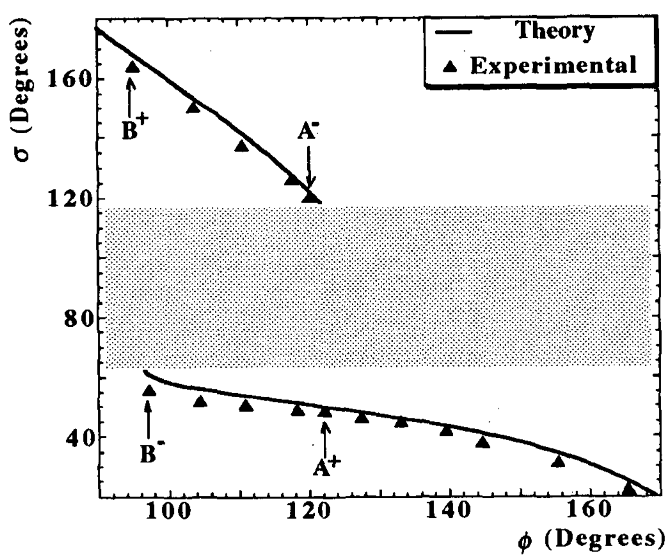

Fig. 10. ϕ versus σ.

VIII. EXPERIMENTAL RESULTS

This section gives experimental results showing switching time bifurcations in the single phase equivalent of the static VAR compensator installed near Rimouski, Quebec [20, ch. 6]. This compensator is a three phase delta connected thyristor controlled reactor and ungrounded wye-connected capacitor banks interfaced to a 230 kV system through a step down transformer as shown in Fig. 9.

This experiment used a 115 V, 60 Hz ac line which was assumed to be a stiff and harmonic free source. The circuit components were scaled as shown in Table I. The reactance to resistance ratio was measured as ≈20 for the inductors and ≈70 for the capacitor. The control circuit used a zero voltage detector synchronized directly across the ac line and a firing pulse generator to build a train of equally spaced firing pulses. The firing pulses are delayed by a time delay generator and transmitted to the back-to-back thyristor modules through a pair of fiber optics. The thyristors used were Westinghouse model 707408 rated 1000 V and 200 A.

Fig. 10 shows how the conduction time σ varies as the phase ϕ is varied. The solid line is computed using (16) and (17) from Section XI and the triangles show the experimental measurements. The solution at point A^- is lost when the thyristor firing is slightly increased and the system state converges to a new steady state at point A^+. This instability occurs when the thyristor conduction time is suddenly decreased due to the appearance of a new earlier current zero. The steady-state solution at point B$^-$ is lost when the thyristor firing phase is slightly decreased upon which the system converges to a new steady state at point B$^+$. This instability occurs when the thyristor turn off time is suddenly increased due to the disappearance of the thyristor current zero.

In this example, the switching time bifurcations are associated with the two natural frequencies of the circuit (the thyristor fully on and fully off) spanning the third harmonic. For example, when the short circuit MVA of the system is infinite ($X_s = 0$), the two natural frequencies do not span the 3rd harmonic and the bifurcation instabilities are absent.

IX. Poincaré Map

The Poincaré map of the static VAR system can be computed by integrating the system equations and taking into account a change in coordinates when the switchings occur. The thyristor turn on time is controlled by the phase parameter ϕ which specifies the delay of the firing pulse. The thyristor turn off occurs when the thyristor current decreases through zero. The thyristors are modeled as short circuits when on and open circuits when off.

The system state vector $x(t)$ specifies the thyristor current, capacitor voltage and the source current:

$$x(t) = \begin{pmatrix} I_r(t) \\ V_c(t) \\ I_s(t) \end{pmatrix}$$

The system input $u(t)$ is the source voltage function shown in Fig. 1. $u(t)$ is assumed to be periodic with period T. During the conducting time of each of the thyristors, the system dynamics are described by the following set of linear differential equations

$$\dot{x} = Ax + Bu \tag{1}$$

where

$$A = \begin{pmatrix} -R_r L_r^{-1} & L_r^{-1} & 0 \\ -C^{-1} & 0 & C^{-1} \\ 0 & -L_s^{-1} & -R_s L_s^{-1} \end{pmatrix} \text{ and } B = \begin{pmatrix} 0 \\ 0 \\ L_s^{-1} \end{pmatrix}.$$

During the off time of each thyristor, the circuit state is constrained to lie in the plane $I_r = 0$ of zero thyristor current. In this mode, the system state vector $y(t)$ specifies the capacitor voltage and the source current:

$$y(t) = \begin{pmatrix} V_c(t) \\ I_s(t) \end{pmatrix}$$

and the system dynamics are given by the linear system

$$\dot{y} = PAP^t y + PBu \tag{2}$$

where P is the projection matrix $P = \begin{pmatrix} 0 & 1 & 0 \\ 0 & 0 & 1 \end{pmatrix}$.

Fig. 11 describes the system dynamics as the system state evolves over a period T. A thyristor starts conducting at time ϕ_0. This mode as described by (1) ends when the thyristor current goes through zero at time $\phi_0 + \sigma_1$. The nonconducting mode as described by (2) follows the conducting mode and continues until the next firing pulse is applied at time ϕ_1. This starts a similar on-off cycle which lasts until the next period starts at time $\phi_0 + T$.

ON (A, B)	OFF (PAP^t, PB)	ON (A, B)	OFF (PAP^t, PB)	
ϕ_0	$\phi_0 + \sigma_1$	ϕ_1	$\phi_1 + \sigma_2$	$\phi_0 + T$
$\longleftarrow T_1 \longrightarrow$		$\longleftarrow T_2 \longrightarrow$		

Fig. 11. System dynamics from time ϕ_0 to $\phi_0 + T$.

The state at the switch on time ϕ_0 is denoted either by the vector $y(\phi_0)$ or by the vector $x(\phi_0)$. These representations of the state at the switch on time are related by

$$x(\phi_0) = P^t y(\phi_0). \tag{3}$$

Equation (3) expresses the fact that the x representation of the state at a switch on is computed from the y representation by adding a new first component which has value zero.

The state at the switch off time $\phi_0 + \sigma_1$ is similarly denoted either by $x(\phi_0 + \sigma_1)$ or $y(\phi_0 + \sigma_1)$ and these are related by

$$y(\phi_0 + \sigma_1) = Px(\phi_0 + \sigma_1). \tag{4}$$

The matrix P in (4) may be thought of as projecting the vector x onto the plane of zero thyristor current.

Given a time interval $[s_1, s_2]$, it is convenient to write $f(\cdot, s_1, s_2)$ for the map which advances the state at s_1 to the state at s_2. For example, a Poincaré map which advances the state by one period T starting at the switch on time ϕ_0 may be written $f(y(\phi_0), \phi_0, \phi_0 + T)$. (If the time s_2 at the end of the interval is a switching time, then there is ambiguity about whether $f(\cdot, s_1, s_2)$ evaluates to $y(s_2)$ or $x(s_2)$. We adopt the convention that $f(x(s_1), s_1, s_2)$ evaluates to $x(s_2)$ and $f(y(s_1), s_1, s_2)$ evaluates to $y(s_2)$. For example, the Poincaré map $f(y(\phi_0), \phi_0, \phi_0 + T)$ evaluates to $y(\phi_0 + T)$.) If the thyristor is on during all of the time interval $[s_1, s_2]$, we write $f(x(s_1), s_1, s_2)$ as $f_{\text{on}}(x(s_1), s_1, s_2)$ and if the thyristor is off during $[s_1, s_2]$, we write $f(y(s_1), s_1, s_2)$ as $f_{\text{off}}(y(s_1), s_1, s_2)$. $f_{\text{on}}(x(s_1), s_1, s_2)$ or $f_{\text{off}}(y(s_1), s_1, s_2)$ can be computed by integrating the corresponding linear system (1) or (2) over the time interval $[s_1, s_2]$.

Now we construct in stages an expression for the Poincaré map $f(y(\phi_0), \phi_0, \phi_0 + T)$ in terms of f_{on} and f_{off} and the coordinate changes (3) and (4). At the start of the period at time ϕ_0, the state is expressed in the y coordinates as $y(\phi_0)$ or, using (3), is expressed as $x(\phi_0) = P^t y(\phi_0)$ in the x coordinates. The state $x(\phi_0 + \sigma_1)$ is obtained by integrating the on linear system (1) with initial state $P^t y(\phi_0)$ from time ϕ_0 to $\phi_0 + \sigma_1$:

$$\begin{aligned} x(\phi_0 + \sigma_1) &= f_{\text{on}}(P^t y(\phi_0), \phi_0, \phi_0 + \sigma_1) \\ &= e^{A\sigma_1} \left(P^t y(\phi_0) + \int_0^{\sigma_1} e^{-A\tau} Bu(\tau + \phi_0) d\tau \right). \end{aligned} \tag{5}$$

The switch off time $s_{\text{off}} = \phi_0 + \sigma_1$ is determined by an equation including P which constrains the thyristor current to be zero:

$$0 = (I - P^t P)x(s_{\text{off}}) = \begin{pmatrix} I_r(s_{\text{off}}) \\ 0 \\ 0 \end{pmatrix} \tag{6}$$

The coordinate change (4) at the switch off and integration of the off linear system (2) yields

$$y(\phi_1) = f_{\text{off}}(Px(\phi_0+\sigma_1), \phi_0+\sigma_1, \phi_1). \quad (7)$$

A half cycle map is given by combining (5) and (7):

$$f(y(\phi_0),\phi_0,\phi_1) = f_{\text{off}}(Pf_{\text{on}}(P^t y(\phi_0),\phi_0,\phi_0+\sigma_1),\phi_0+\sigma_1,\phi_1).$$

The Poincaré map may now be written by composing two successive half cycle maps and then neglecting the gory details of the time arguments:

$$f(y(\phi_0),\phi_0,\phi_0+T) = f(f(y(\phi_0),\phi_0,\phi_1),\phi_1,\phi_0+T) \quad (8)$$
$$= f_{\text{off}}Pf_{\text{on}}P^t f_{\text{off}}Pf_{\text{on}}P^t(y(\phi_0)). \quad (9)$$

X. Stability of Periodic Solutions

When the static VAR circuit is in steady state with a periodic trajectory of period T, the Poincaré map has a corresponding fixed point. That is,

$$f(y(\phi_0),\phi_0,\phi_0+T) = y(\phi_0).$$

The stability of the periodic orbit can be computed from the Jacobian of the Poincaré map evaluated at the fixed point [10], [25], [26]. In particular, the periodic orbit is exponentially stable if the eigenvalues of the Jacobian lie inside the unit circle. Since the thyristor turn off time s_{off} and the Poincaré map are discontinuous at a switching time bifurcation [22], [6], we assume when computing the Jacobian in this section that the system is not exactly at a switching time bifurcation.

To compute the Jacobian of the Poincaré map, we first compute the Jacobian of maps which advance the state from the beginning to the end of a time interval containing one switching. Let $[t_1,t_2]$ be a fixed time interval including a thyristor turn on at time s_{on} and no other switchings. The map $f(y(t_1),t_1,t_2)$ advances the state $y(t_1)$ to the state $x(t_2)$ and we want to compute the Jacobian $Df(y(t_1),t_1,t_2)$ which is a 3×2 matrix.

$$f(y(t_1),t_1,t_2) = f_{\text{on}}(P^t f_{\text{off}}(y(t_1),t_1,s_{\text{on}}),s_{\text{on}},t_2)$$
$$= e^{A(t_2-s_{\text{on}})}P^t e^{PAP^t(s_{\text{on}}-t_1)}y(t_1) + \text{function}(\,s_{\text{on}},t_1,t_2\,).$$

Differentiating with respect to $y(t_1)$ and keeping in mind that the thyristor turn on time s_{on} is a fixed quantity (recall that the thyristor firing is equidistant), we obtain

$$Df(y(t_1),t_1,t_2) = e^{A(t_2-s_{\text{on}})}P^t e^{PAP^t(s_{\text{on}}-t_1)}. \quad (10)$$

Let $[t_2,t_3]$ be a fixed time interval including a thyristor turn off at time s_{off} and no other switchings. The map $f(x(t_2),t_2,t_3)$ advances the state $x(t_2)$ to the state $y(t_3)$ and we want to compute the Jacobian $Df(x(t_2),t_2,t_3)$ which is a 2×3 matrix.

$$f(x(t_2),t_2,t_3) = f_{\text{off}}(Pf_{\text{on}}(x(t_2),t_2,s_{\text{off}}),s_{\text{off}},t_3)$$
$$= e^{PAP^t(t_3-s_{\text{off}})}Pe^{A(s_{\text{off}}-t_2)} \cdot \left[x(t_2) + \int_{t_2}^{s_{\text{off}}} e^{A(t_2-\tau)}Bu(\tau)d\tau\right]$$
$$+ \int_{s_{\text{off}}}^{t_3} e^{PAP^t(t_3-\tau)}PBu(\tau)d\tau. \quad (11)$$

Differentiating with respect to $x(t_2)$ and keeping in mind that the thyristor turn off time s_{off} is a function of $x(t_2)$, we obtain

$$Df(x(t_2),t_2,t_3) = e^{PAP^t(t_3-s_{\text{off}})}Pe^{A(s_{\text{off}}-t_2)} + e^{PAP^t(t_3-s_{\text{off}})}PA(I-P^tP) \cdot e^{A(s_{\text{off}}-t_2)}\left[x(t_2) + \int_{t_2}^{s_{\text{off}}} e^{A(t_2-\tau)}Bu(\tau)d\tau\right]Ds_{\text{off}} \quad (12)$$

Note that the two terms associated with s_{off} in the limits of the two integrals of (11) cancel. The row vector Ds_{off} is the gradient of s_{off} with respect to $x(t_2)$. The second term of (12) may be written as

$$e^{PAP^t(t_3-s_{\text{off}})}PA(I-P^tP)x(s_{\text{off}})Ds_{\text{off}}$$

which vanishes according to the constraint equation (6) so that we obtain the surprising and simple result

$$Df(x(t_2),t_2,t_3) = e^{PAP^t(t_3-s_{\text{off}})}Pe^{A(s_{\text{off}}-t_2)}. \quad (13)$$

Result (13) implies that the switch off time may be regarded as constant when deriving the Jacobian.

The map advancing the state over the combined interval $[t_1,t_3]$ can be written as the composition

$$f(y(t_1),t_1,t_3) = f(f(y(t_1),t_1,t_2),t_2,t_3)$$

and the chain rule yields

$$Df(y(t_1),t_1,t_3) = Df(x(t_2),t_2,t_3)Df(y(t_1),t_1,t_2)$$

so that substitution from (10) and (13) gives

$$Df(y(t_1),t_1,t_3) = e^{PAP^t(t_3-s_{\text{off}})}Pe^{A(s_{\text{off}}-s_{\text{on}})}P^t e^{PAP^t(s_{\text{on}}-t_1)}.$$

In particular, let $t_1 = s_{\text{on}} = \phi_0$, $s_{\text{off}} = \phi_0+\sigma_1$, $t_3 = \phi_1$ and $T_1 = \phi_1 - \phi_0$ to obtain the Jacobian of the half cycle map:

$$Df(y(\phi_0),\phi_0,\phi_1) = e^{PAP^t(T_1-\sigma_1)}Pe^{A\sigma_1}P^t. \quad (14)$$

Applying the chain rule to (8) and using (14) for the Jacobians of the half cycle maps yields the 2×2 Jacobian of the Poincaré map:

$$Df(y(\phi_0),\phi_0,\phi_0+T) = e^{PAP^t(T_2-\sigma_2)}Pe^{A\sigma_2}P^t e^{PAP^t(T_1-\sigma_1)}Pe^{A\sigma_1}P^t. \quad (15)$$

One of the interesting and useful consequences of (15) is that the stability of the periodic orbit only depends on the state and the input via σ_1 and σ_2. It is remarkable that (15) is also the formula that would be obtained for fixed switching times σ_1 and σ_2; the varying switching times apparently introduce no additional complexity in the formula, but the nonlinearity of the circuit is clear since σ_1 and σ_2 vary as a function of $y(\phi_0)$.

XI. Simplification for Symmetric Periodic Orbits

It is convenient to take advantage of symmetry when the periodic orbits are half wave symmetric. Half wave symmetry of a periodic orbit means that the thyristor firing pulses are sent every half cycle and the orbit is half wave symmetric. In particular, the two conduction times $\sigma_1 = \sigma_2 = \sigma$ are equal. Moreover, the system states at the half cycle are equal in magnitude and opposite in sign to the system states at the beginning of the cycle. That is, if $y(\phi_0)$ is the system state at the beginning of the period, then:

$$f(y(\phi_0), \phi_0, \phi_0 + T/2) = -y(\phi_0). \quad (16)$$

The conduction time σ of the conducting thyristor is given by the constraint equation

$$0 = (I - P^t P)x(\phi_0 + \sigma). \quad (17)$$

The fixed points $y(\phi_0)$ corresponding to half wave symmetric periodic orbits can be computed by solving (16) and (17) simultaneously. In addition, the Poincaré map Jacobian in (15) simplifies to:

$$Df(y(\phi_0), \phi_0, \phi_0 + T) = \left(e^{PAP^t(T/2-\sigma)} P e^{A\sigma} P^t\right)^2. \quad (18)$$

XII. Conventional Bifurcations

We review the instabilities expected from conventional bifurcation theory. The thyristor controlled reactor circuit becomes a discrete time nonlinear system when analyzed with the Poincaré map. Conventional bifurcation theory (e.g., [10], [25]) describes several typical ways in which a discrete time nonlinear system can become unstable as parameters vary. The system is assumed to be initially operating in a stable periodic fashion before the bifurcation occurs and the nature of the bifurcation is determined by where a critical eigenvalue of the Jacobian of the Poincaré map crosses the unit circle. (The stable periodic orbit disappears in a fold bifurcation if an eigenvalue crosses the unit circle at 1, becomes modulated with another frequency or becomes unstable in a Niemark or secondary Hopf bifurcation if a complex conjugate pair of eigenvalues crosses the unit circle and period doubles if an eigenvalue crosses the unit circle at -1.) Several authors (e.g., [4], [3], [21]) have investigated instabilities such as Hopf and period doubling bifurcations in averaged models of fast switching power electronic circuits.

The Jacobian formula (18) can be used to rule out conventional bifurcations of half wave symmetric periodic orbits in the thyristor controlled reactor circuit. The Jacobian in (18) is a complicated function of the initial state $y(\phi_0)$ and the input $u(t)$, but it only depends on $y(\phi_0)$ and $u(t)$ via the switching time σ. Thus to determine stability, it is only necessary to test the stability of the Jacobian in (18) as σ varies over its range of 0 to 180°. Numerical computation of the eigenvalues of the Jacobian in (18) as σ varies over this range as shown in Fig. 12 indicates that the absolute values of the eigenvalues are less than 0.98 for both the simulation and the experimental examples. This demonstrates that, for the given component values, the circuits do not lose stability in a conventional bifurcation. We conclude that the eigenvalues of

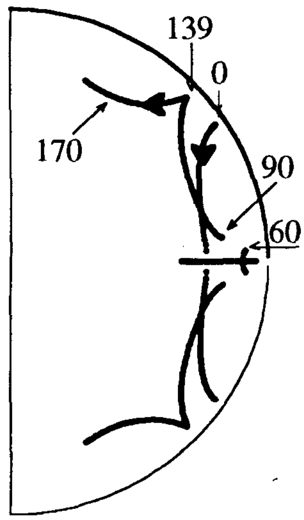

Fig. 12. Eigenvalues of Jacobian as σ varies.

the Jacobian of the Poincaré map are strictly inside the unit circle as a switching time bifurcation is approached; that is, the eigenvalues give no warning of the switching time bifurcation. The points in the eigenvalue locus of Fig. 12 at which an eigenvalue approaches the unit circle can be predicted and associated with resonance effects; see [5].

The switching time bifurcation can be detected as a zero gradient of the thyristor current at the switch off time; what may be surprising is that this zero gradient has no effect on the Jacobian. As a thyristor current zero disappears in a fold bifurcation, the gradient of the thyristor current evaluated at the current zero tends to zero and one might expect this to influence the Jacobian. In particular, the gradient of the thyristor current tending to zero implies that the sensitivity Ds_{off} of the switch off time with respect to the initial state becomes infinite. If the Jacobian contained a term including Ds_{off} (*cf.* (12)), at least one eigenvalue of Df would leave the unit circle and a conventional bifurcation would occur before the switching time bifurcation was encountered. However, this analysis is wrong because the Jacobian simplification shows that the term in the Jacobian involving Ds_{off} vanishes (*cf.* the vanishing of the second term of (12)). Thus the Jacobian simplification ensures that the fold bifurcation of the thyristor current is not expressed in the eigenvalues of the Jacobian and that the switching time bifurcation will occur. See [6] for a more rigorous explanation. In the case of a switching time bifurcation in which a new thyristor current zero appears, the gradient at the thyristor current zero *before* the bifurcation does not become zero as the bifurcation occurs and the Jacobian is unaffected by the bifurcation.

XIII. Conclusion

This paper studies instabilities in a thyristor controlled reactor circuit used for reactive power control of power systems in which switching times change suddenly, or bifurcate as a system parameter (phase of the thyristor firing) varies slowly. The switching time bifurcations are explained and their mechanisms are illustrated by simulation and experiment. In particular, we have shown how distortion of current waveforms can cause a thyristor switch off time to disappear or a new thyristor switch off time to suddenly appear by fold bifurcations of the thyristor current. The consequence of the sudden change in switch off time is that stable periodic operation of the circuit is lost and a transient occurs. These switching time bifurcations are not explained by the analysis of thyristor controlled reactor circuits with average inductor models. Nor are the switching time bifurcations explained by the conventional theory of bifurcations in which stability is lost when eigenvalues of the Jacobian matrix cross the unit circle.

The thyristor controlled reactor circuit is a nonlinear, periodically operated circuit. The Poincaré map can be computed by integrating the system equations and taking into account a change in coordinates when switchings occur. We have derived a simple formula for the Jacobian of the Poincaré map (also see [18], [6]). This Jacobian describes the stability of the steady state periodic operation of the circuit under an open loop equidistant firing pulse control. In particular, the Jacobian formula is used to demonstrate numerically that none of the conventional bifurcations occur in our circuit examples. For simulation evidence of switching time bifurcations in a single phase thyristor controlled series capacitor circuit see [13] and [15].

This paper makes progress in describing and understanding instabilities in a nonlinear thyristor controlled reactor circuit with a simple topology. However, despite the simple topology, we expect that this circuit may well contain other novel behaviors. One of our objectives is to develop new ways of understanding and computing instabilities of general switching circuits by first studying in detail the thyristor controlled reactor circuit. The genericity of fold bifurcations suggests that switching time bifurcations describe typical ways in which general switching circuits with thyristors become unstable.

REFERENCES

[1] L. J. Bohmann and R. H. Lasseter, "Harmonic interactions in thyristor controlled reactor circuits," *IEEE Trans. Power Delivery*, vol. 4, pp. 1919–1926, July 1989.

[2] *Current activity in flexible AC transmission systems*, IEEE Publication 92 TH 0465-5 PWR, Apr. 1992.

[3] J. H. B. Deane and D. C. Hamill, "Instability, subharmonics and chaos in power electronics systems," *IEEE Trans. Power Electron.*, vol. 5, pp. 260–268, July 1990.

[4] J. H. B. Deane, "Chaos in a current-mode controlled boost dc-dc convertor," *IEEE Trans. Circuits Syst. — I*, vol. 39, pp. 680–683, Aug. 1992.

[5] I. Dobson, S. G. Jalali, and R. Rajaraman, "Damping and resonance in a high power switching circuit," in *Systems and Control Theory for Power Systems*, J. H. Chow, P. V. Kokotovic, and R. J. Thomas, Eds., IMA vol. 64 in *Mathematics and Its Applications*. New York: Springer Verlag, 1995, pp. 137-156.

[6] I. Dobson, "Stability of ideal thyristor and diode switching circuits," *IEEE Trans. Circuits Syst. — I*, vol. 42, pp. 517–529, Sept. 1995.

[7] H. W. Dommel, "Digital computer solutions of electromagnetic transients in single and multiphase networks," *IEEE Trans. Power Apparat. Syst.*, vol. PAS-88, pp. 388–399, Apr. 1969.

[8] EPRI Report ELP4541PCCMP, vol. 1 and 2; *The Electromagnetic Transients Program (EMTP), Version 1.0, Revised Rule Book*, Apr. 1986.

[9] M. Grötzbach and R. von Lutz, "Unified modeling of rectifier-controlled DC-power supplies," *IEEE Trans. Power Electron.*, vol. 1, pp. 90–100, Apr. 1986.

[10] J. Guckenheimer and P. Holmes, *Nonlinear Oscillations, Dynamical Systems and Bifurcations of Vector Fields*. New York: Springer-Verlag, 1986.

[11] L. Gyugyi, "Power electronics in electric utilities: Static var compensators," *Proc. IEEE*, vol. 76, pp. 483–494, Apr. 1988.

[12] S. G. Jalali and R. H. Lasseter, "Harmonic interaction of power systems with static switching circuits," *Power Electronics Specialists Conf.*, June 1991, M.I.T., MA, pp. 330-337.

[13] ——, "Harmonic instabilities in advanced series compensators," in *EPRI FACTS Conf.*, Boston, MA, May 1992, in *Electric Power Research Institute Report* TR-101784.

[14] S. G. Jalali, I. Dobson, and R. H. Lasseter, "Instabilities due to bifurcation of switching times in a thyristor controlled reactor," in *Power Electronics Specialists Conf.*, Toledo, Spain, July 1992, pp. 546-552.

[15] S. G. Jalali, "Harmonics and Instabilities in thyristor based switching circuits," Ph.D. dissertation, Univ. Wisconsin-Madison, 1993.

[16] S. G. Jalali, R. H. Lasseter, and I. Dobson, "Dynamic response of a thyristor controlled switched capacitor," *IEEE Trans. Power Delivery*, vol. 9, pp. 1609–1615, July 1994.

[17] P. T. Krein, J. Bentsman, R. M. Bass, and B. C. Lesieutre, "On the use of averaging for the analysis of power electronic systems," *IEEE Trans. Power Electron.*, vol. 5, pp. 182–190, Apr. 1990.

[18] J. P. Louis, "Non-linear and linearized models for control systems including static convertors," in *Proc. Third Int. Federation Automat. Contr. Symp. Contr. Power Electron. Elect. Drives*, Lausanne, Switzerland, Sept. 1983, pp. 9–16.

[19] R. D. Middlebrook and S. Cuk, "A general unified approach to modeling switching power converter stage," in *IEEE Power Electron. Specialists Conf.*, 1976, pp. 18–34.

[20] T. J. E. Miller, Ed. *Reactive Power Control in Electric Systems*. New York: Wiley, 1982.

[21] S. Pavljasevic, D. Maksimovic, "Using a discrete-time model for large-signal analysis of a current-programmed boost convertor," in *Power Electronics Specialists Conf.*, June 1991, M.I.T., MA, pp. 715-721.

[22] R. Rajaraman, I. Dobson, and S. Jalali, "Nonlinear dynamics and switching time bifurcations of a thyristor controlled reactor," *IEEE Intl. Symp. Circuits Syst.*, Chicago, IL, May 1993, pp. 2180–2183.

[23] S. R. Sanders, J. M. Noworolski, X. Z. Liu, and G. C. Verghese, "Generalized averaging method for power conversion circuits," *IEEE Trans. Power Electron.*, vol. 6, pp. 251–259, Apr. 1991.

[24] F. D. Tan and R. S. Ramshaw, "Instabilities of a boost converter system under large parameter variations," *IEEE Trans. Power Electron.*, vol. 4, pp. 442–459, Oct. 1989.

[25] J. M. T. Thompson and H. B. Stewart, *Nonlinear Dynamics and Chaos: Geometrical Methods for Scientists and Engineers*. London: Wiley, 1986, reprinted 1987.

[26] G. C. Verghese, M. E. Elbuluk, and J. G. Kassakian, "A general approach to sampled-data modeling for power electronic circuits," *IEEE Trans. Power Electron.*, vol. 1, pp. 76–89, Apr. 1986.

[27] R. Yacamini and J.W. Resende, "Thyristor controlled reactors as harmonic sources in HVDC converter stations and AC systems," *IEE Proc.*, Part B, vol. 133, pp. 263–269, July 1986.

Sasan Jalali received the B.S., M.S., and Ph.D. degrees in electrical engineering in 1988, 1990, and 1993, respectively, from the University of Wisconsin-Madison.

He joined Siemens Energy and Automation, Atlanta, GA, in 1993. His interests include nonlinear effects in utility power electronics and the analysis and development of flexible ac transmission systems.

Ian Dobson received the B.A. degree in mathematics from Cambridge, England in 1978 and the Ph.D. degree in electrical engineering from Cornell University, NY in 1989.

He worked for five years as a systems analyst for the British firm EASAMS Ltd.; this included simulation of switching circuits for plasma physics power supplies on contract to Culham Laboratory, UKAEA, England. He is now an associate professor of electrical engineering with the University of Wiscnsin-Madison. His current interests are applications of bifurcation theory and nonlinear dynamics, voltage collapse in electric power systems and utility power electronics.

Robert H. Lasseter received the Ph.D. degree in physics from the University of Pennsylvania, Philadelphia, in 1971.

He was a Consultant Engineer with the General Electric Company until 1980 when he joined the University of Wisconsin-Madison. His main interest is the application of power electronics to utility systems including hardware, methods of analysis and simulation.

Dr. Lasseter became a Fellow of the IEEE Power Engineering Society in 1992.

Giri Venkataramanan received the B.E. degree from the University of Madras, India, in 1986, the M.S. degree from the California Institute of Technology, Pasadena in 1987 and the Ph.D. degree from the University of Wisconsin-Madison in 1992, all in electrical engineering.

Currently he is an Assistant Professor of electrical engineeering at Montana State University, Bozeman. His interests include modeling, design and control of power conversion systems and the introduction of pragmatism into engineering education.